Determination of the Magnetic Symmetry of Hexagonal Manganites by Second Harmonic Generation

M. Fiebig,[1] D. Fröhlich,[1] K. Kohn,[2] St. Leute,[1] Th. Lottermoser,[1] V. V. Pavlov,[3] and R. V. Pisarev[3]

[1]*Institut für Physik, Universität Dortmund, 44221 Dortmund, Germany*

[2]*Department of Physics, Waseda University, 3-4-1 Okubo, Shinjuku-ku, Tokyo 169-8555, Japan*

[3]*Ioffe Physical Technical Institute of the Russian Academy of Sciences, St. Petersburg 194021, Russia*

(Received 16 February 2000)

Optical second harmonic spectroscopy is introduced as a powerful supplement for the determination of complex magnetic structures. Experimental efforts are simplified and new degrees of freedom are opened. Thereby, some principal or technical restrictions of neutron or magnetic x-ray diffraction experiments are overcome. High spatial resolution leads to additional information about magnetically ordered matter. As an example, the noncollinear magnetic structure of the hexagonal manganites $R\mathrm{MnO_3}$ (R = Sc, Y, Ho, Er, Tm, Yb, Lu) is analyzed. The results show that some earlier conclusions on their magnetic symmetry and properties should be revised.

PACS numbers: 75.25.+z, 42.65.Ky, 75.50.Ee, 78.20.Ls

The determination of symmetry is a prerequisite for any detailed evaluation of phononic, electronic, and magnetic properties of matter. From symmetry, fundamental selection rules and conservation laws are derived which are then applied in the microscopic description of many-body systems. Diffraction experiments with the use of x rays, electrons, and neutrons have proved to be powerful tools for studying the symmetry and structure of matter. In general, however, diffraction experiments do not allow the complete determination of the crystallographic point and space groups. Auxiliary macroscopic techniques are therefore required [1]. The determination of the magnetic structure is an even more challenging task. Apart from recent magnetic x-ray diffraction experiments [2], neutron diffraction has remained the only practical method for deriving the magnetic point and space groups [3,4].

In practice, neutron diffraction experiments are subject to several restrictions [3]. Large samples have to be used which ideally should not only be in a single-crystalline but also in a magnetic single-domain state. These criteria are often difficult to meet, and powdered samples are used. Data treatment becomes even more complicated in the case of complex noncollinear arrangements of spins. Different magnetic structures may be indistinguishable, particularly if unpolarized neutron beams are applied. Again, auxiliary information is indispensable. In many cases, magnetic, magnetoelectric, and magneto-optical measurements can be employed, but due to their integral character conclusions on the microscopic magnetic structure remain difficult.

Recently, nonlinear optical methods, and in particular second harmonic generation (SHG), have been applied in magneto-optics. In most cases, SHG was used for studying the static and dynamic properties of specific ferromagnets and antiferromagnets with simple crystallographic and magnetic structures [5–8]. However, a profound investigation of the applicability of nonlinear spectroscopy to a broad range of magnetically ordered materials of potentially different structure is still overdue. In this Letter we show that nonlinear optical spectroscopy meets this purpose and therefore qualifies as an important supplement to neutron experiments for the study of magnetically ordered materials. Principal or technical restrictions of the diffraction experiments are overcome, which can simplify the determination of magnetic structure, and may even lead to results which cannot be gained by the existing techniques. New degrees of freedom are opened which provide additional information about magnetic phases.

The hexagonal manganites $R\mathrm{MnO_3}$ (R = Sc, Y, Ho, Er, Tm, Yb, Lu) provide a very instructive example to test the method and to disclose its advantages. At room temperature, the structure of these compounds is described by the crystallographic space group $P6_3cm$ [9]. A phase transition to the antiferromagnetic state occurs at $T_N \sim 70$–130 K [10,11]. The magnetic properties arise from the $\mathrm{Mn^{3+}}(3d^4)$ ions with spin $S = 2$. For Ho, Er, Tm, and Yb, there are additional contributions to the magnetic properties from the rare-earth ions with the possibility of $4f$ spin ordering below $\sim$6 K [12]. For clarity, we restrict the discussion to triangular antiferromagnetic ordering of the $\mathrm{Mn^{3+}}$ spins (Fig. 1), since other possible arrangements [13–15] have not been observed so far. The two models in Fig. 1 are distinguished by parallel (α) or antiparallel (β) orientation of corresponding spins at $z = 0$ and $z = c/2$ in the unit cell. Depending on the angle φ between the magnetic moment and the x axis [16] being 0°, 90°, or in between for both α and β models, this leads to six possible magnetic symmetries.

In principle, several nonlinear optical methods can be used for studying magnetic structures. It will be seen that SHG as the lowest-order nonlinear process can already distinguish between all the possible spin structures. The determination of magnetic structures from SHG is based on the relation between the induced nonlinear polarization $P_i(2\omega)$ and the electric field components $E_j(\omega)$ and

 0031-9007/00/84(24)/5620(4)$15.00

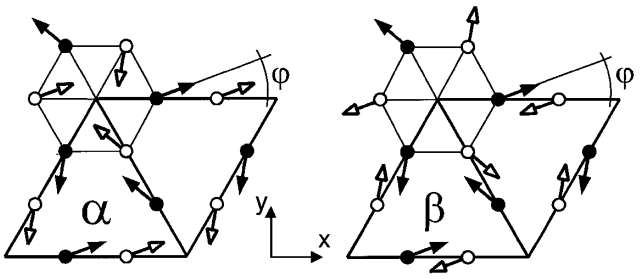

FIG. 1. Planar triangular magnetic structures of hexagonal $R\mathrm{MnO_3}$. A projection of the Mn spins at $z = 0$ (closed arrows) and $z = c/2$ (open arrows) on the xy plane of the magnetic unit cell shows parallel (α model) or antiparallel orientation (β model) of neighboring spins on one line. The axes perpendicular to the glide planes c (mirror planes m) are the x (y) axes. The sixfold axis is the z axis [1].

$E_k(\omega)$ of the fundamental light:

$$P_i(2\omega) = \epsilon_o(\chi^{(i)}_{ijk} + \chi^{(c)}_{ijk})E_j(\omega)E_k(\omega), \qquad (1)$$

where $\chi^{(i)}_{ijk}$ and $\chi^{(c)}_{ijk}$ are the crystallographic and magnetic SHG susceptibility tensor components, respectively. In the electric-dipole approximation both are polar third-rank tensors, but $\chi^{(i)}_{ijk}$ is time invariant, whereas $\chi^{(c)}_{ijk}$ is time noninvarint which originates in the breaking of time-reversal symmetry by the spin ordering. The tensor components $\chi^{(i)}_{ijk}$ and $\chi^{(c)}_{ijk}$ are uniquely defined by the crystallographic and magnetic space groups, respectively [17]. They can be identified experimentally by measuring the intensity of the SH signal $I(2\omega) \propto |P_i(2\omega)|^2$ for various directions and polarizations of the incident and emitted light. The nonvanishing magnetic tensor components $\chi^{(c)}_{ijk}$ for the six space groups derived from Fig. 1 are given in Table I. The selection rules are all different and therefore allow the unambiguous assignment of the magnetic symmetry. This was impossible before, since neutron experiments could not discriminate between α- and β-type spin arrangements [3,10]. Although the SHG is a macroscopic method, it can distinguish between the different magnetic space groups ($P\underline{6}_3\underline{c}m$ and $P\underline{6}_3c\underline{m}$) of one magnetic point group ($\underline{6}m\underline{m}$), since the x and y crystalline axes are uniquely defined (Fig. 1).

In our experiments, both polished and unpolished flux-grown (0001) platelets [18] of x-ray oriented $R\mathrm{MnO_3}$ single crystals with thicknesses of 0.05–0.4 mm and lateral dimensions of 1–3 mm were used. Low-temperature absorption measurements revealed that with the exception of some narrow lines attributed to electronic transitions between $4f$ levels of the rare-earth ions [19] all samples are transparent below 1.5 eV, which allows one to choose a transmission setup. Samples were illuminated by 5 mJ, 3 ns light pulses with a photon energy of 1.0–1.5 eV and at a repetition rate of 10–40 Hz. Wave plates and optical and polarizing filters were used to set the polarization of the incoming light, separate the fundamental and the SH light behind the sample, and analyze the polarization of the SH signal. A telephoto lens was used to project the signal light on a cooled CCD camera where it was integrated in spectroscopic or spatially resolved in topographic experiments [20,21].

Figure 2 shows the SH spectra of $\mathrm{HoMnO_3}$ and the angular and temperature dependence of the SH intensity for light incident along the optical axis ($k \parallel z$). The polar graphs were recorded by projecting the component of the SH light oriented parallel to the polarization of the incident light while rotating this polarization by 360°. These plots allow the samples to be oriented with an error $<0.5°$ in the xy plane. The presence of a strong signal for $k \parallel z$ immediately restricts the choice between six possible spin structures to the three α configurations since only these show a SH component which couples x or y polarized incident and SH light. For the β model, a longitudinal z polarized wave is always involved (Table I) which cannot propagate outside the crystal. At Néel temperature the SH signal vanishes, which confirms its purely magnetic origin. In the temperature range between $T_N = 72$ K and $T_R = 41$ K, the SH signal exhibits a sixfold symmetry with maximum intensity for $P(2\omega) \parallel E(\omega) \parallel x$ and zero intensity for $P(2\omega) \parallel E(\omega) \parallel y$. The corresponding magnetic symmetry is thus $P\underline{6}_3\underline{c}m$ with $\chi^{(c)}_{xxx} \neq 0$ and $\chi^{(c)}_{yyy} = 0$. Below the reorientation temperature T_R, the SH spectrum is quite different and the polar dependence of the signal is rotated by 30° with respect to the high-temperature phase. This corresponds to $\chi^{(c)}_{xxx} = 0$ and $\chi^{(c)}_{yyy} \neq 0$ and therefore to the magnetic space group $P\underline{6}_3c\underline{m}$. The change of magnetic structure goes along with a 90° spin rotation and a change of the antiferromagnetic domain structure. In a narrow temperature interval around T_R, both $\chi^{(c)}_{xxx}$ and $\chi^{(c)}_{yyy}$ are nonvanishing due to the lower $P\underline{6}_3$ symmetry in the

TABLE I. Magnetic selection rules for hexagonal $R\mathrm{MnO_3}$. Triples ijk denote the components of the SH tensor $\chi^{(c)}_{ijk}$. $\oplus$ denotes the sum of the 0° and 90° components.

	φ in Fig. 1	Space group	Selection rules for magnetic SHG
α_1	0°	$P\underline{6}_3c\underline{m}$	$yxx = xyx = xxy = -yyy$
α_2	90°	$P\underline{6}_3\underline{c}m$	$xyy = yxy = yyx = -xxx$
α_φ	0°...90°	$P\underline{6}_3$	$\alpha_1 \oplus \alpha_2$
β_1	0°	$P6_3\underline{cm}$	$xyz = xzy = -yxz = -yzx$
β_2	90°	$P6_3cm$	$xxz = xzx = yyz = yzy, zzz, zxx = zyy$
β_φ	0°...90°	$P6_3$	$\beta_1 \oplus \beta_2$

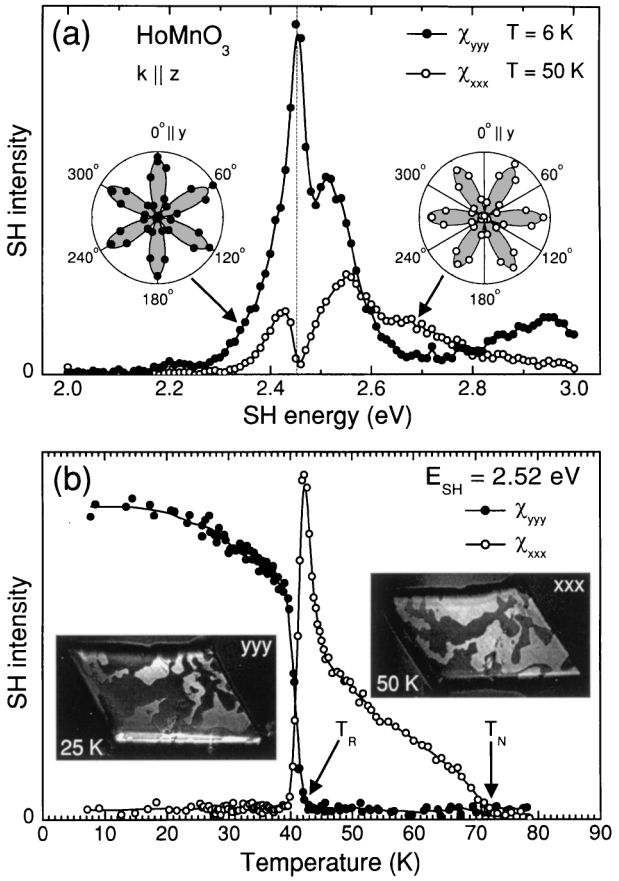

FIG. 2. Spectral, angular, and temperature dependence of the $\chi^{(c)}_{xxx}$ (open circles) and the $\chi^{(c)}_{yyy}$ components (closed circles) of the SH tensor.

course of the spin rotation. The spin reorientation was also observed by neutron diffraction [10], but only now the unambiguous assignment to the space groups of the α model could be made. Note that only spectroscopic *and* temperature dependence considered provides the full information needed for the determination of the magnetic structure. The temperature dependence can reveal the various magnetic phases and the nonvanishing magnetic and nonmagnetic SH tensor components. However, only the SH spectrum reveals the photon energy with a suitable SH signal from the investigated magnetic sublattice. In particular, the identification of vanishing SH tensor components can only be made spectroscopically, in order to exclude an accidental absence of SH at some energy.

Furthermore, the magnetic SH spectrum of $YMnO_3$ at $T < T_N$ exactly resembles that of $HoMnO_3$ in the low-temperature phase, whereas the magnetic SH spectrum of $ErMnO_3$ resembles that of $HoMnO_3$ in the high-temperature phase. A microscopic understanding of the spectra is not even needed to assign a $P\underline{6}_3c\underline{m}$ structure to $YMnO_3$ and a $P\underline{6}_3\underline{c}m$ structure to $ErMnO_3$ from this observation [16]. Spectroscopy can be regarded as an additional degree of freedom which may further support the symmetry analysis—or, in this case, unnecessitate the need for sample orientation by other techniques.

$ScMnO_3$ offers the most intriguing results. Figure 3 shows a series of spatially resolved SH images of a $ScMnO_3$ sample at various temperatures with the SH light being due to the $\chi^{(c)}_{xxx}$ and $\chi^{(c)}_{yyy}$ components. Just below $T_N = 123$ K, we find $\chi^{(c)}_{xxx} \neq 0$ and $\chi^{(c)}_{yyy} = 0$ for the whole sample which corresponds to a $P\underline{6}_3\underline{c}m$ symmetry. In the 62–22 K range, the spins in the red region rotate by 90°, the symmetry now being $P\underline{6}_3c\underline{m}$ with $\chi^{(c)}_{xxx} = 0$ and $\chi^{(c)}_{yyy} \neq 0$. Note that although the borderline of this transition moves across the sample with temperature, locally the full 90° rotation occurs immediately, once the local reorientation temperature is reached. Below 22 K, the green region, too, exhibits a spin reorientation. In this region, the angle φ between spins and x axes increases with decreasing temperature, but contrary to the red region, the full 90° rotation is not accomplished. At 1.5 K, φ varies between 72° at the lower right corner near the blue region and ~30° at the opposite border with the red region. Because of the lower $P\underline{6}_3$ symmetry, both $\chi^{(c)}_{xxx}$ and $\chi^{(c)}_{yyy}$ are nonvanishing. The remaining blue region is not at all affected by the transition and retains the $P\underline{6}_3\underline{c}m$ symmetry down to 1.5 K. We thus find a coexistence of three magnetic phases in one single crystal. Although the physical background behind this coexistence is not the topic of this Letter, our observations already indicate a high sensitivity of the magnetic structure to sample inhomogeneities (most likely strain). Previous experiments revealed only a sequence of gradual spin reorientations

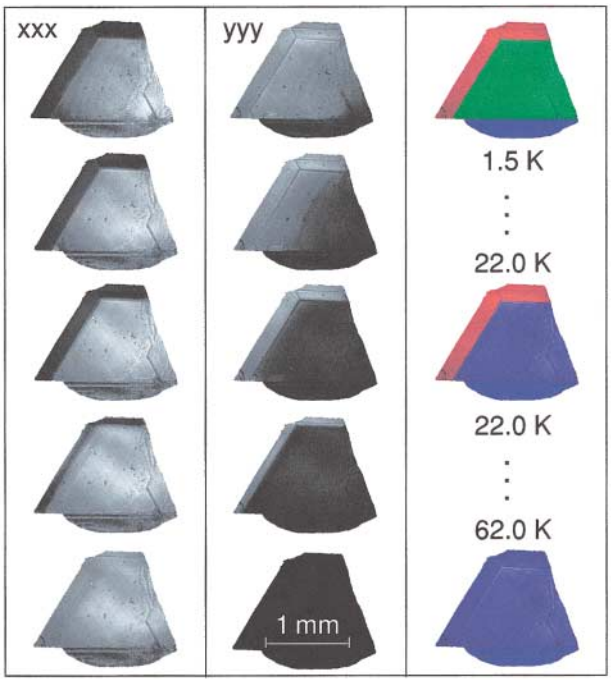

FIG. 3 (color). Spatially resolved magnetic SH images of $ScMnO_3$ for various temperatures below $T_N = 123$ K. Each pair of black-and-white pictures was exposed with SH light at 2.44 eV from the $\chi^{(c)}_{xxx}$ (label *xxx*) and the $\chi^{(c)}_{yyy}$ (label *yyy*) tensor components. Red, green, and blue areas mark regions with $P\underline{6}_3c\underline{m}$, $P\underline{6}_3$, and $P\underline{6}_3\underline{c}m$ symmetry, respectively.

averaged across the sample [22]. The SH experiment, however, provides an abundance of information about the coexistence of different antiferromagnetic phases and gradual or abrupt transitions between them, which is derived from just another degree of freedom, that is, spatial resolution.

Figure 4 summarizes the symmetries of all the hexagonal $R\mathrm{MnO_3}$ compounds as derived from the SHG experiments. First, all compounds belong to the α model with parallel orientation of corresponding spins in the $z = 0$ and $c/2$ planes. A weak ferromagnetic moment, which was reported elsewhere [11,22], could not be confirmed. Note that the SHG based symmetry analysis is not obscured by ferromagnetic $\mathrm{Mn_3O_4}$ impurities as conventional magnetization experiments are. Second, the low $P\underline{6}_3$ symmetry with φ between 0° and 90° was observed in $\mathrm{ScMnO_3}$, but similar results on $\mathrm{ErMnO_3}$ and $\mathrm{TmMnO_3}$ [10] could not be confirmed. Finally, the absence of a SH signal above T_N for light incident along the z axis is consistent with a $P6_3cm$, but not with a $P3c1$ symmetry in the paramagnetic state. Uncertainties in former diffraction experiments [9,11] prevented the ultimate clarification of the crystal structure so far.

In conclusion, it was shown that nonlinear optical spectroscopy is an important complement to the neutron and x-ray based investigation of magnetic matter in several aspects. By analyzing the polarization dependent spectra arising from magnetic contributions to nonlinear optical susceptibilities (i) magnetic structures known from other measurements could be proved or disproved, (ii) magnetic structures which were indistinguishable in neutron diffraction could be distinguished, and (iii) spectral and spatial resolution as additional degrees of freedom could be applied to overcome some of the principal or technical restrictions of the existing techniques. Nonlinear spectroscopy allows the topographical and sublattice sensitive determination of magnetic symmetry with a high degree of discrimination between similar magnetic structures. In this Letter, only SH transmission experiments are discussed, the application of which are limited to noncentrosymmetrical transparent crystals. In case of centrosymmetric or highly absorbing materials and surface magnetic layers, higher nonlinearities and reflection spectroscopy have to be applied [23]. For instance, first magnetic three-photon difference-frequency experiments revealed a coupling between antiferromagnetic and charge ordering in one of the colossal magnetoresistive perovskite manganites [24].

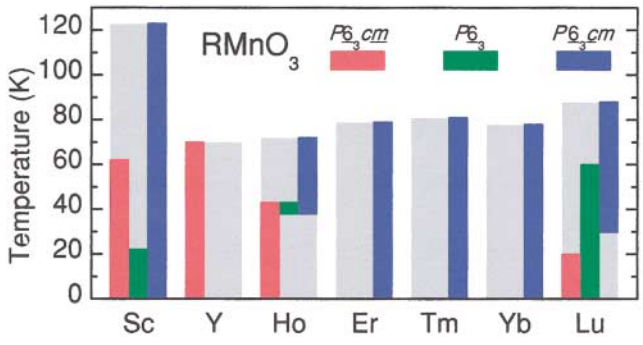

FIG. 4 (color). Magnetic symmetry of the hexagonal manganites. Sc, Ho, and Lu show a coexistence of magnetic phases with temperature intervals being sample specific. Intervals are thus given for a single sample. Rare-earth spin ordering below 6 K was not taken into account.

This work was supported by the Deutsche Forschungsgemeinschaft and the Alexander-von-Humboldt-Stiftung.

[1] *International Tables for X-Ray Crystallography, Vol. A: Space-Group Symmetry,* edited by T. Hahn (Reidel Publishing Company, Boston, 1987).
[2] W. G. Stirling and M. J. Cooper, J. Magn. Magn. Mater. **200**, 755 (1999).
[3] G. E. Bacon, *Neutron Diffraction* (Clarendon Press, Oxford, 1975).
[4] P. J. Brown, Physica (Amsterdam) **192B**, 14 (1993).
[5] *Nonlinear Optics in Metals*, edited by K. H. Bennemann (Clarendon Press, Oxford, 1998).
[6] M. Fiebig, D. Fröhlich, B. B. Krichevtsov, and R. V. Pisarev, Phys. Rev. Lett. **73**, 2127 (1994).
[7] D. Fröhlich, S. Leute, V. V. Pavlov, and R. V. Pisarev, Phys. Rev. Lett. **81**, 3239 (1998).
[8] D. Fröhlich, S. Leute, V. V. Pavlov, R. V. Pisarev, and K. Kohn, J. Appl. Phys. **85**, 4762 (1999).
[9] H. L. Yakel, W. C. Koehler, E. F. Bertaut, and E. F. Forrat, Acta Crystallogr. **16**, 957 (1963).
[10] W. C. Koehler, H. L. Yakel, E. O. Wollan, and J. W. Cable, in *Proceedings of the 4th Conference on Rare-Earth Research, Phoenix, Arizona, 1964* (Gordon and Breach, New York, 1965), pp. 63–75; Phys. Lett. **9**, 93 (1964).
[11] H. W. Xu, J. Iwasaki, T. Shimizu, H. Sato, and N. Kamegashira, J. Alloys Compd. **221**, 274 (1995).
[12] N. Iwata and K. Kohn, J. Phys. Soc. Jpn. **67**, 3318 (1998).
[13] E. F. Bertaut, M. Mercier, and R. Pauthenet, J. Phys. (Paris) **25**, 550 (1964).
[14] G. M. Nedlin, Sov. Phys. Solid State **6**, 2156 (1964).
[15] W. Sikora and V. N. Syromyatnikov, J. Magn. Magn. Mater. **60**, 199 (1986).
[16] Axes in this paper are chosen in accordance with Ref. [1]. Previous assignments have to be adapted since they are based on the 122 magnetic point groups which do not distinguish between the α_1 and α_2 models.
[17] R. R. Birss, *Symmetry and Magnetism* (North-Holland, Amsterdam, 1966).
[18] B. Wanklyn, J. Mater. Sci. **7**, 813 (1972).
[19] G. H. Dieke, *Spectra and Energy Levels of Rare Earth Ions in Crystals* (Interscience Publishers, New York, 1968).
[20] M. Fiebig, D. Fröhlich, S. Leute, and R. V. Pisarev, Appl. Phys. B **66**, 265 (1998).
[21] S. Leute, T. Lottermoser, and D. Fröhlich, Opt. Lett. **24**, 1520 (1999).
[22] M. Bieringer and J. E. Greedan, J. Solid State Chem. **143**, 132 (1999).
[23] M. Trzeciecki, A. Dähn, and W. Hübner, Phys. Rev. B **60**, 1144 (1999).
[24] M. Fiebig *et al.* (unpublished).